OH + Isoprene: A Direct Dynamics Study

Jihye Jeon,[a] John R. Barker,[b] and Kihyung Song[a,*]

[a] Department of Chemistry, Korea National University of Education, Cheongju, Chungbuk, Republic of Korea

[b] Department of Climate and Space Sciences and Engineering University of Michigan, Ann Arbor, MI, USA

[a] Korea National University of Education
[b] University of Michigan
* Corresponding Author: ksong@knue.ac.kr

This is the author manuscript accepted for publication and has undergone full peer review but has not been through the copyediting, typesetting, pagination and proofreading process, which may lead to differences between this version and the Version of Record. Please cite this article as doi: 10.1002/bkcs.11145

ABSTRACT

The products and mechanisms active in the isoprene + OH reaction were investigated using the direct dynamics method. High energies were used in order to identify every possible reaction channel. The trajectories were classified as dissociative and non-dissociative, depending on whether fragmentation occurred during the 4 ps time window of the simulations. The non-dissociative trajectories were further classified as radical additions, rearrangements, and cyclizations. The most dominant category was the addition of OH to the carbons of isoprene to form adducts. Some adducts react further by isomerization and cyclization. The dissociative trajectories were classified as hydrogen abstractions, substitutions, and eliminations. Among these, the dominant category was direct hydrogen abstraction to produce H_2O and a free radical. At higher energies, more reaction was observed. In simulations at 300K, the only reaction category observed was OH addition to the double bonds in isoprene to form adducts.

1. Introduction

Isoprene (2-methyl-1,3-butdiene, C_5H_8) is one of the most abundant volatile organic compounds (VOCs) emitted by plants, and a precursor of atmospheric ozone and secondary organic aerosols (SOAs).[1-10] Isoprene reacts rapidly with with hydroxyl radical (OH), ozone, NO_3 free radicals, and other atmospheric constituents.[3,8,9,11-14] When isoprene reacts with OH in the presence of O_2, peroxy radicals are produced. In turn, the peroxy radicals can react with nitric oxide (NO) to produce nitrogen dioxide (NO_2), which leads to the production of ozone when photolyzed.[5,9,10] Therefore, isoprene plays a significant role in ozone production.[2-5,8,10,11,14-17]

The detailed mechanism by which isoprene reacts with OH radicals is now at least partly understood, although very complex. It is known that an OH radical can add to either end of either double C=C bond to produce any of four different free radical intermediates. It is also thought that OH can abstract a hydrogen atom from any of the five carbons, although the methyl hydrogens are the most vulnerable. Much work, both experimental and theoretical, has been directed at quantitatively characterizing these reactions. Because the reaction system is so complex, the interpretation of experimental data and the strategies followed in the theoretical studies have been guided largely by chemical intuition and by analogy with simpler

reaction systems. Thus the danger always exists that a significant reaction path will be overlooked. Direct dynamics, which is the subject of this paper, is a theoretical technique the makes it possible to investigate the broad features of a complex reaction system in order to identify all of the reaction paths, which subsequently can be studied in more depth with other techniques.

Nguyen et al.[18,19] used direct dynamics along with other methods to investigate the kinetics and pressure dependence of the ethene + NO_3 reaction system. They used direct dynamics simulations to identify the major product sets: oxirane (C_2H_4O) + NO_2, NO + $2CH_2O$, and hydroxyethyl radical + NO_2, and then they investigated the potential energy surface in more detail. From master equation simulations, they obtained rate constants and branching ratios.

In the present study, direct dynamics simulations are used to investigate the isoprene + OH reaction in order to identify the major pathways. The simulations were performed by using quasi-classical trajectories[24] (implemented in program VENUS[25]) and a force field computed on the fly by MSINDO,[26] a semi-empirical quantum chemistry code. The computational methods used in this study are described in the next section. Results and discussion are presented in the third section,

followed by Conclusions in the last section.

2. Computational Methods

In order to determine the reaction channels and probabilities of each channel of the isoprene + OH reaction, quasi-classical trajectory (QCT) calculations were performed using VENUS[25] coupled with the semiempirical quantum chemistry program, MSINDO.[26] Due to quantum chemical instability (SCF convergence failure) of the free radical system, it was not possible to use faster quantum chemistry programs such as MOPAC.[27] The relative translational energies were chosen to be 30 and 50 kcal/mol. These energies are much higher than found in ambient atmospheric conditions, but they were chosen to be high enough so that significant amounts of fragmentation and rearrangement reactions could be observed during the limited simulated time period of 4 ps. In these high energy simulations, a 300 K Boltzmann distribution was used for both the vibrational and rotational energies of isoprene. For the OH radical, the initial vibrational quantum number was set to zero and the rotational quantum number was set to 4, which is the most probable value at 300 K.

In separate batches, trajectory calculations were also performed with a 300K Maxwell-Boltzmann translational energy distribution to simulate

atmospheric conditions. In these thermal simulations, the initial internal vibrational and rotational energies and corresponding momenta of the reactants were sampled from 300 K Boltzmann distributions.

Potential energies and gradients were obtained on the fly from the MSINDO program suite. Trajectories were initiated at 10 Å center of mass distance and ran for 4 ps or until the distance between OH and isoprene reached 15 Å. The Velocity Verlet integration method[28] with a 0.2 fs time step was used to integrate the classical equations of motion. The impact parameter, b, was chosen randomly with b_{max} set to 4 Å. Batches consisting of ~10^4 trajectories were simulated for each set of initial conditions. Animation of each trajectory was visualized to determine the structures of products and reaction mechanisms.

Structures and energies of reactants and major products produced in the trajectory calculations were determined using MSINDO[26] and the Gaussian 09 program.[29] The MSINDO program was used for all of the trajectory calculations. For comparison, geometries were fully optimized at the UB3LYP/6-311+G(d,p) level and single point energies were calculated at the CBS-QB3 and G3B3 levels of theory. Products and reaction mechanisms were determined by visualizing the trajectory.

The chemical reaction cross section[30] for the i^{th} reaction channel was calculated using Eq. 1:

$$\sigma_i(E) = \pi \cdot b_{max}^2 \cdot P_i \qquad (1)$$

where b_{max} is the maximum impact parameter (4 Å) and P_i is the reaction probability of the i^{th} channel, obtained from the number N_i of trajectories that reacted via the i^{th} channel and N_{total} the total number of trajectories in a given batch: $P_i = N_i/N_{total}$. In the simulations initiated with a delta function of initial energy (E), the rate constant[30] for each reaction channel was obtained by

$$k_i(E) = \sigma_i(E) \cdot v \qquad (2)$$

where v is the relative velocity corresponding to the relative translational energy $E_{rel} = \frac{1}{2}\mu v^2$ and μ is the reduced mass of isoprene and OH.

For the Boltzmann translational distribution, the thermal average velocity was used instead.

$$k_i(T) = (8k_BT/\pi\mu)^{\frac{1}{2}} \cdot \pi b_{max}^2 \cdot P_i \qquad (3)$$

When bond cleavage occurs, quantum chemistry programs often have difficulties on the location of unpaired electron due to the multi-reference effects, and it could go to excited electronic states. Hence, some trajectories

had poor energy conservation or terminated abnormally. Such trajectories were discarded and not used in calculating P_i.

3. Results and Discussion

Thermochemistry

How well does MSINDO[26] compare with more accurate methods? MSINDO was used in these direct dynamics calculations because it is at least qualitatively accurate. Fig 1 shows the optimized structures obtained using MSINDO, which are in reasonable agreement with those obtained using methods like CBS-QB3[33] and the G3B3[34] method with UB3LYP/6-311+G(d,p). Relative energies will be given later in Table I.

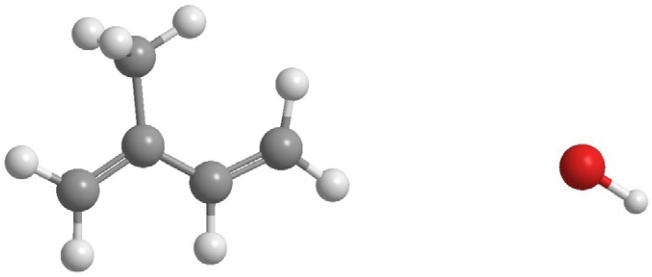

Figure 1. Optimized structures for isoprene and OH. The white, gray and red spheres represent hydrogen, carbon and oxygen atoms, respectively.

The reactions of OH with isoprene have been investigated in many

previous studies and much is known. For example, OH can simply add to each of the the four doubly-bonded carbon atoms, producing four distinct hydroxyalkyl radical products. OH radicals can also abstract an H-atom from the methyl group. The latter is consistent with a related study,[43] which showed that OH addition reactions are common for unsaturated hydrocarbons, because such reactions have low energy thresholds for addition to double bonds, while saturated compounds (alkanes, alcohols, ethers, esters and carbonyls), which have no double bonds, undergo hydrogen abstraction reactions at higher energies. However, at very high energies, such as in this study, hydrogen abstraction of strongly bonded olefinic hydrogen atoms is also possible.

The first four reactions are expected to produce free radical complexes, but those complexes are energized and may react further by isomerization and fragmentation during the 4 ps time window. In order to categorize the reactions and reaction products, the isoprene carbons and hydrogens were labeled according to the numbering scheme in Figure 2. Labels C1 and H1 designate the carbon at site #1 and the hydrogen atoms, attached to C1, respectively, and so forth for all of the atoms in isoprene.

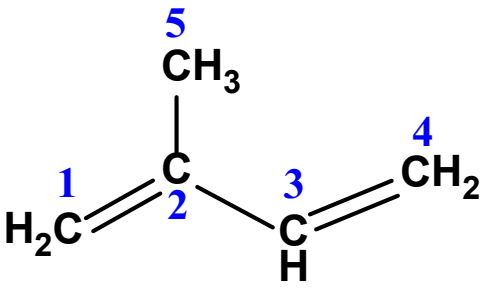

Figure 2. Numbering of carbon atoms in isoprene.

Table 1 shows the single point energies calculated for the dominant products, which are labeled according to the above numbering scheme and identified fully in subsequent sections of the paper. The energies were obtained by CBS-QB3[33] and the G3B3[34] method with UB3LYP/6-311+G(d,p) optimized geometries and compared to MSINDO optimized energies. For future ab initio direct dynamics studies,[35] the UB3LYP/6-31G* method was also used for optimized energies. Energies are relative to the reactant energy for each method and zero-point energy corrected values are given in parentheses.

Relative energies computed using CBS-QB3 and G3B3 are generally consistent with previous work [5,36], as shown in Table 2. The values obtained using MSINDO were not in good agreement with those of high level theories such as CBS-QB3 and G3B3 but are comparable to the relatively low level theory values obtained using UB3LYP/6-31G(d), which is used

often for direct dynamics studies.[37-40] The mean absolute error of MSINDO relative to G3B3 and UB3LYP/6-31G(d) for species AC1 and AC4 are 18.8 and 15.5 kcal/mol, respectively.

Table 1. Energies (kcal/mol) of major products relative to OH + isoprene[a]

Species	MSINDO	UB3LYP[b]	UB3LYP[c]	CBS-QB3[d]	G3B3[d]
AC1	-58.10 (-54.80)	-43.41 (-39.53)	-39.83 (-35.98)	-39.52 (35.69)	-37.33 (-33.45)
AC2	-44.78 (-42.08)	-25.18 (-22.78)	-21.87 (-19.56)	-25.75 (-23.46)	-25.54 (-23.14)
AC3	-43.21 (-40.61)	-25.76 (-23.19)	-22.58 (-20.04)	-24.89 (-22.37)	-24.14 (-21.56)
AC4	-50.39 (-47.09)	-40.76 (-36.99)	-36.94 (-33.16)	-37.09 (-33.33)	-35.00 (-31.21)
AC2R	-54.96 (-51.26)	-34.29 (-30.62)	-30.92 (-27.24)	-30.50 (-26.84)	-29.85 (-26.18)
AC3R	-48.31 (-44.71)	-32.11 (-28.36)	-28.82 (-25.20)	-28.73 (-25.12)	-28.01 (-24.26)
DH1 + H_2O	-6.64 (-9.04)	2.02 (1.58)	-4.45 (-4.83)	-6.83 (-7.21)	-5.00 (-5.45)
DH3 + H_2O	-16.46 (-19.26)		-16.87 (-18.49)	-17.75 (-19.38)	
DH4 + H_2O	-7.05 (-9.45)	4.33 (3.43)	-2.08 (-2.95)	-4.96 (-5.83)	-3.54 (-4.45)
DH5 + H_2O	-31.91 (-34.91)	-20.10 (-21.08)	-26.63 (-27.40)	-28.95 (-29.72)	-26.86 (-27.84)

[a]Values in parentheses have been corrected for zero-point energy. [b]Basis set is 6-31G*.
[c]Basis set is 6-311+G(d, p).
[d]Single point calculations performed at the optimized geometries using UB3LYP/6-311+G(d, p).

Table 2. Relative energies (kcal/mol, not including zero point energy) [a]

	UB3LYP[b]	MP2[d]	UB3LYP[c]
AC1	-39.8	-37.3	-47.7
AC2	-21.9	-30.5	-29.7
AC3	-22.6	-29.4	-30.2
AC4	-37.3	-34.3	-45.0

[a]ref 5.
[b] 6-311++G** basis set from ref 5.
[c] 6-311G* basis set from ref 36.
[d]Basis set is 6-31G** from ref 36.

Dissociative and Non-Dissociative Trajectories

For convenience in discussing the collisions between the two reactants, we will regard the isoprene molecule as a target and the OH radical as a projectile. We will also refer to each trajectory as a "collision". Each trajectory was initiated at a distance large enough (10 Å) so that the initial interaction between the colliding pair is negligible. In collisions with impact parameter larger than 3 Å, which is beyond the edge of the isoprene molecule “target”, the collision partners never experience a strong interaction and no chemical reaction occurs; these collisions are "chemically elastic". In collisions with smaller impact parameters, the interaction between the reactants is often large enough for reaction to occur. In order for that to happen, some portion of the initial relative translational energy must be converted to internal energy. This energy release is expected to be somewhat localized in the region of the isoprene molecule that was initially struck by the OH radical. Localized internal energy tends to spread throughout a molecule rapidly by intramolecular vibrational energy redistribution (IVR). At the same time, or course, chemical reaction might be taking place. Typical time scales for IVR are thought to be $\gtrsim$1 ps, but could be as short as ~0.1 ps. During the 4 ps time window of the trajectory simulations, reaction can occur before, during, and after IVR is complete,

resulting in a wide variety of possible reaction products.

In the present work, collisions are pragmatically categorized as "elastic" if after 4 ps separated OH and isoprene are identifiable. "Reactive" collisions can be classified as "dissociative" or "non-dissociative", depending on whether bimolecular products are produced during the 4 ps time window. It is important to recognize that the complexes formed in the non-dissociative collisions cannot survive indefinitely, since energy is conserved and all have enough energy to regenerate the initially separated reactants. Thus the distinction between dissociative and non-dissociative simply depends on whether the lifetime of the complex is greater than 4 ps.

The total percentage of reaction at the initial energy of 30 kcal/mol was 20.38% (from a batch of 10058 trajectories) and 24.59% (from 10140 trajectories) at 50 kcal/mol. Reactive trajectories were further characterized as either "non-dissociative", or "dissociative" (see Table 3 and Figure 3). The results show that trajectories of both types are more likely at higher energy and the proportion of dissociative trajectories increases at higher energy. These results are consistent with previous studies,[5,11,14,22,23,31,32] which found that the HO + isoprene reaction occurs mostly by OH addition to the double bonds of isoprene, yielding highly vibrationally excited hydroxyalkyl radicals.

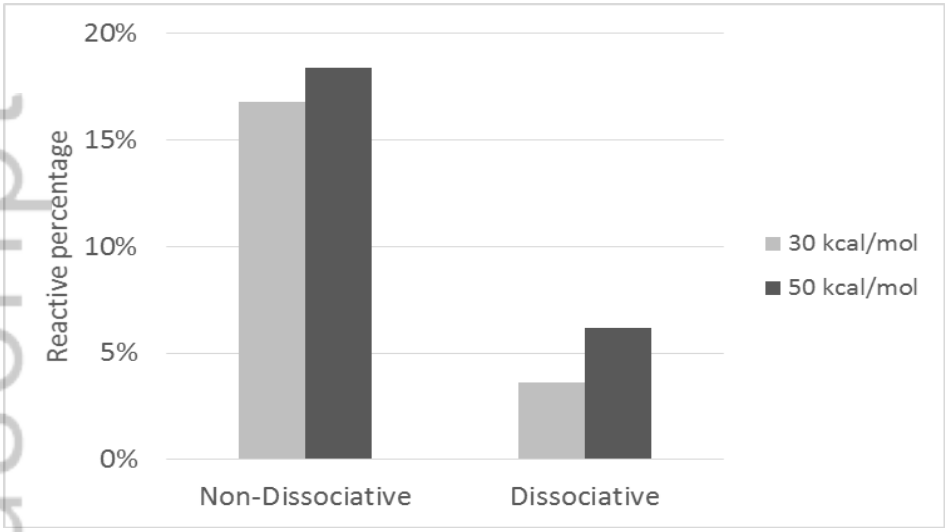

Figure 3. Percentages of Dissociative and Non-Dissociative trajectories.

Table 3. Numbers and percentages of Dissociative and Non-Dissociative trajectories

Initial Energy:	E = 30 kcal/mol	E = 50 kcal/mol
Trajectories	10058	10140
Non-Dissociative	1691 (16.8±0.4)%[a]	1868 (18.4±0.4)%
Dissociative	359 (3.6±0.2)%	625 (6.2±0.2)%

[a] The percentages are given in parentheses with one standard deviation relative error.

To determine the nature of the chemical transformations that take

place in reactive trajectories, every such trajectory was examined and a reaction mechanism was identified. Snapshots of reactive trajectories that are representative of the more important mechanism are shown in Figures 4-6 and in the Supporting Information.

The energies of AC1 and AC4 are about 5-18 kcal/mol lower than the energies of AC2 and AC3. This is due to the fact that AC1 and AC4 are stabilized by allylic resonance, while AC2 and AC3 are not (Figure 7).[4,5,11,13,22,23,36,41]

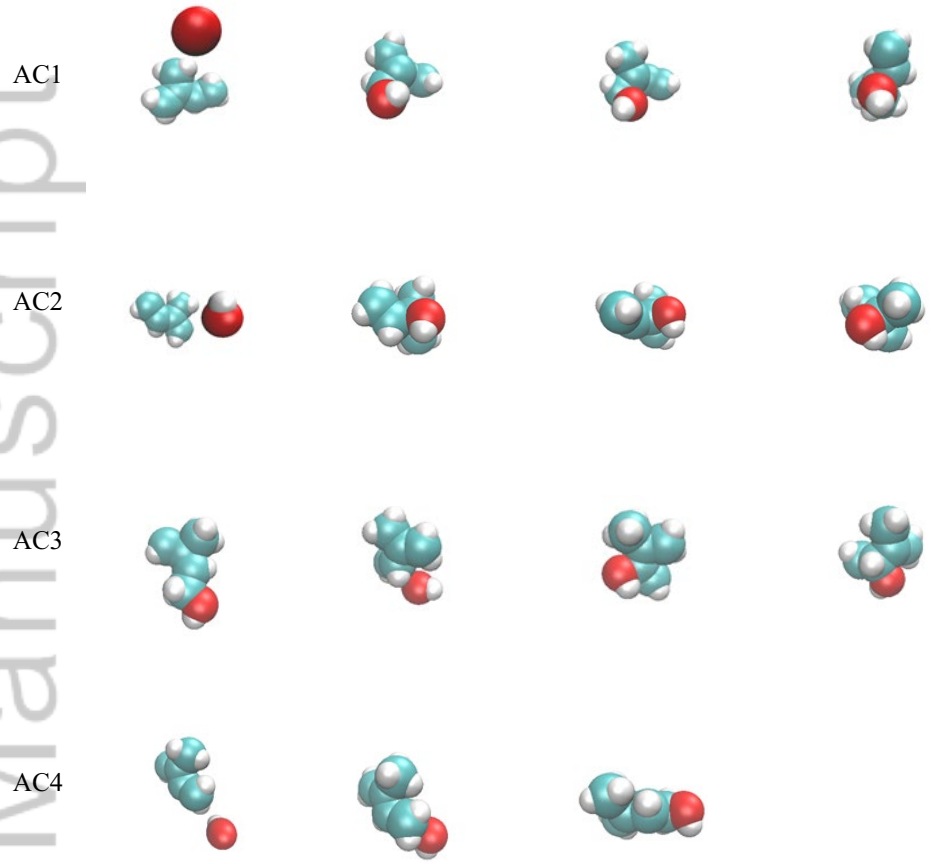

Figure 4. Snapshots of the animations showing the radical additions.

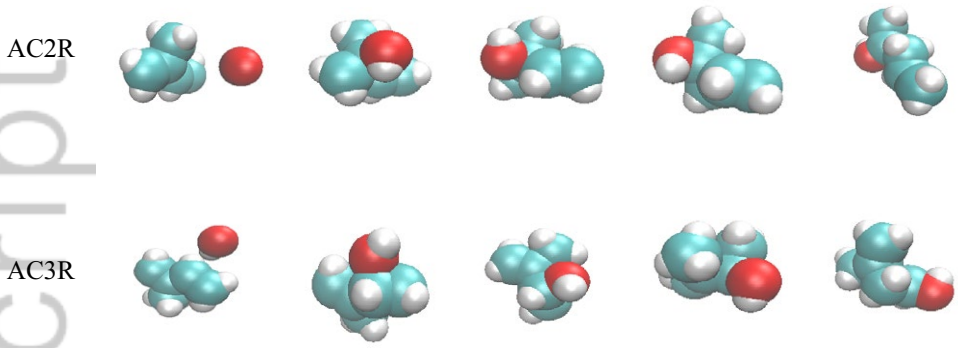

Figure 5. Snapshots of the animations showing the rearrangements with radical additions.

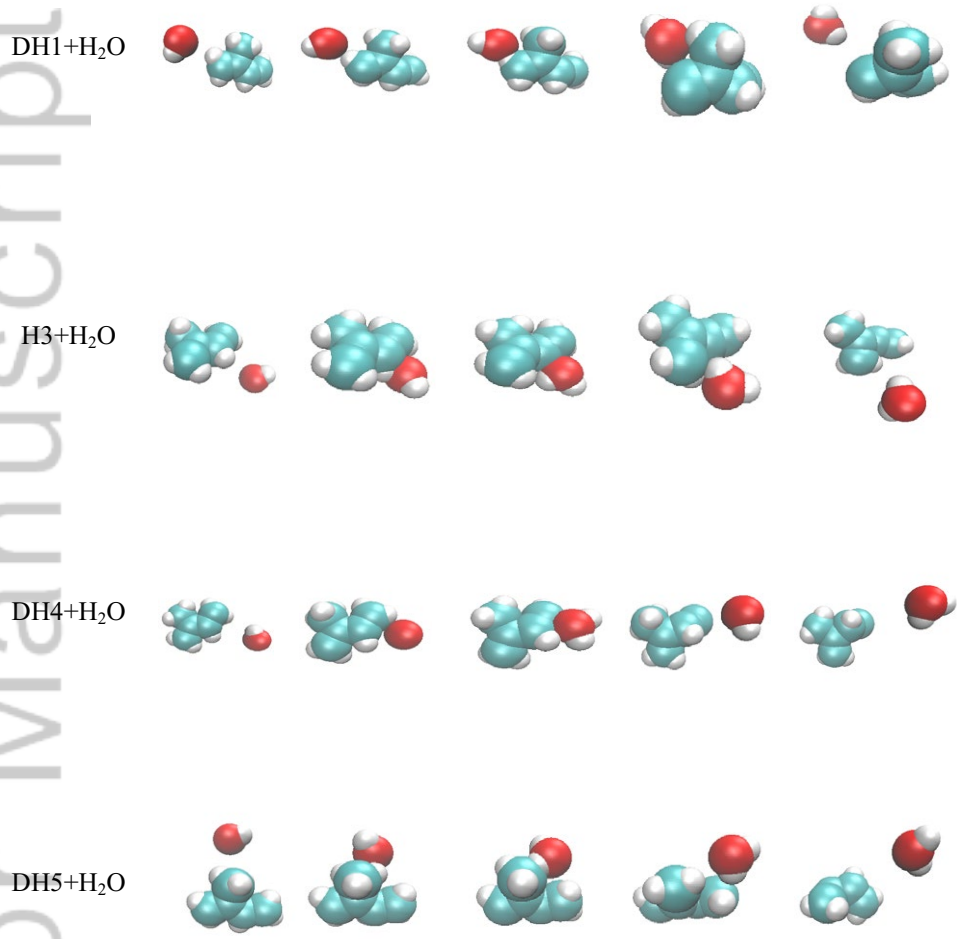

Figure 6. Snapshots of the animations showing hydrogen atom abstractions.

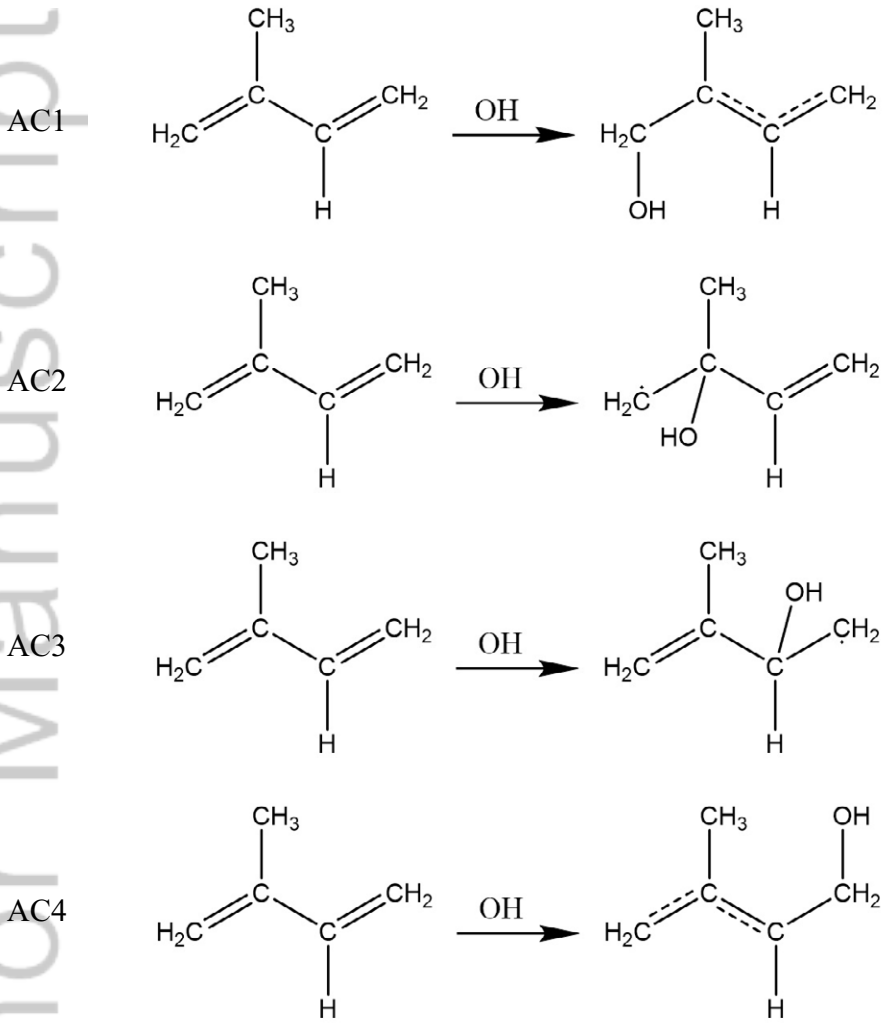

Figure 7. Radical addition mechanism of isoprene + OH reaction.

Isomers AC2R and AC3R are produced by isomerization of the vibrationally excited hydroxyacyl radicals AC2 and AC3. It was found that the rearrangement after addition is observed at sites C2 and C3, but not at

sites C1 and C4, probably because hydroxyacyl radicals AC1 and AC4 are more stable than AC2 and AC3. A more detailed explanation would require knowledge of the transition states and activation energies of the relevant reactions.[5,14,23,42]

The dominant products of the dissociative reactions are water molecules and the free radicals resulting from hydrogen abstraction reactions (DH1, DH3-DH5). This type of reaction usually occurs when OH radical hits a target hydrogen atom directly (Figure 8). As shown in Table 2, the energies of the hydrogen abstraction products are much higher than the association products except that of DH5, where the free radical product is stabilized by resonance, as shown in Figure 7.

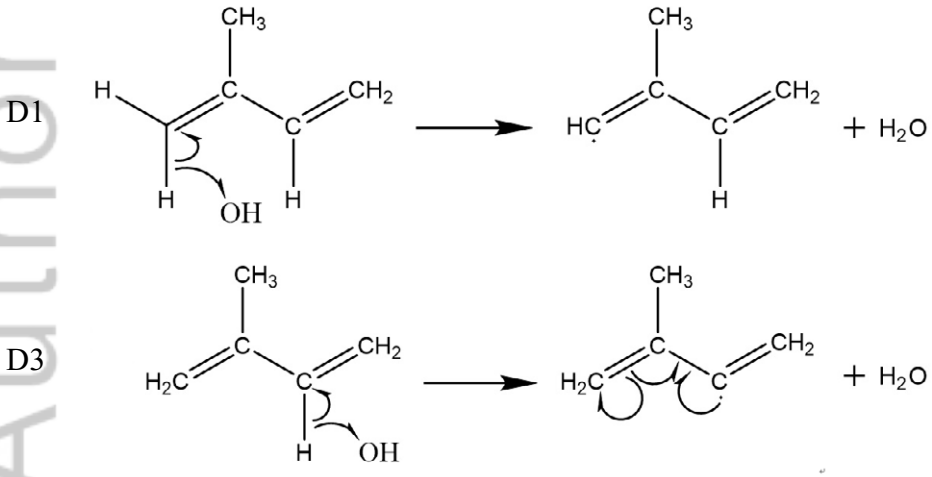

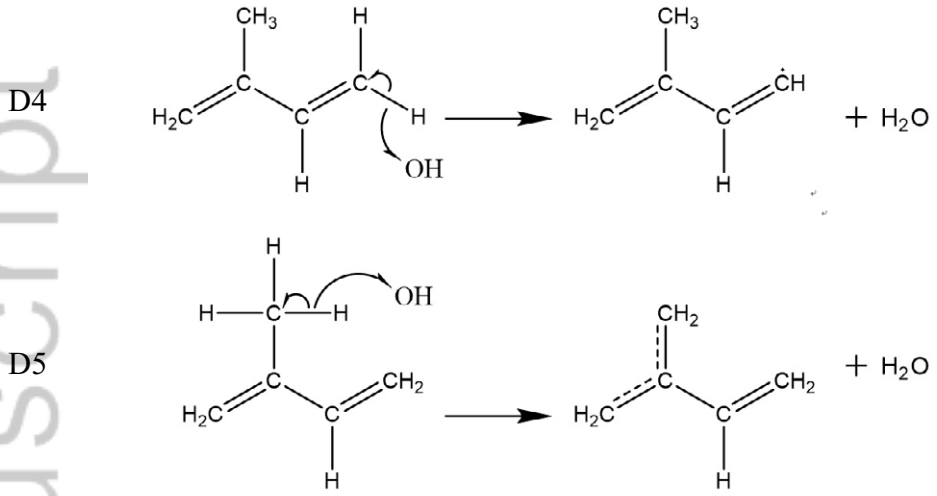

Figure 8. Hydrogen abstraction mechanisms.

Mechanisms

Three general mechanisms are most important:

1. Addition of OH to one of the four doubly-bonded carbon atoms of isoprene (AC1-AC4).
2. Addition of OH to one of the four doubly-bonded carbon atoms, followed by structural rearrangement (AC2R, AC3R). A special sub-category is Cyclization, in which the rearrangement produces a cyclic species.
3. Direct hydrogen atom abstraction by OH from one of the four unique hydrogen atom sites in isoprene (DH1, DH3, DH4, and DH5).

These mechanisms are discussed in the following sub-sections and the

numbers and percentages of all reactive trajectories are summarized and categorized in Table 4. Additional mechanisms of lower probability are also discussed.

Table 4. Non-dissociative Trajectories categorized according to mechanism

Product	E = 30kcal/mol		E = 50kcal/mol	
AC1	569	(5.7 ±0.2)[a]	640	(6.3±0.2)
AC2	147	(1.5±0.1)	128	(1.3±0.1)
AC3	260	(2.6±0.2)	256	(2.5±0.2)
AC4	633	(6.3±0.2)	714	(7.0±0.3)
AC2R	47	(0.5±0.1)	77	(0.8±0.1)
AC3R	24	(0.2±0.1)	32	(0.3±0.1)
AC4R	0	(0.0)	1	(0.01±0.01)
Cyclization	11	(0.11±0.03)	20	(0.20±0.04)
Total	1691	(16.8±0.4)	1868	(18.4±0.4)

[a] The percentage of the total trajectories in a batch is given in parentheses; statistical errors are one standard deviation.

Non-Dissociative Trajectories

These trajectories fall into three groups: radical additions (ACn), addition accompanied by rearrangement (ACnR), and by Cyclizations. All of these mechanisms start with an OH radical addition at one of the four doubly-bonded carbon atom sites. The number of trajectories for each addition site is given in Table 5.

Table 5. **Association site statistics for non-dissociative trajectories**

Association site	E = 30kcal/mol	E = 50kcal/mol
C1	569 (5.7±0.2) [a]	640 (6.3±0.2)
C2	199 (2.0±0.1)	217 (2.1±0.1)
C3	286 (2.8±0.2)	293 (2.9±0.2)
C4	637 (6.3±0.2)	718 (7.1±0.3)
Total	1691 (16.8±0.37)	1868 (18.4±0.4)

[a] The percentage is given in parentheses; statistical errors are one standard deviation.

Radical Addition

Addition of OH to one of the four sites with no further reaction during the 4 ps time window is classified as a Radical Addition. The numbers of trajectories of this type are 1609 (95.2%) out of 1691 reactive trajectories at 30 kcal/mol and 1738 (93.1%) out of 1868 at 50 kcal/mol. Thus most of the non-dissociative reactive trajectories are of this type. The major association sites of OH radical were found to be C1 and C4, probably due to allylic stabilization.

Addition + Rearrangement

When a structural isomerization occurs after radical association, the trajectory is classified as a Rearrangement. When the rearrangement produces a cyclic intermediate, it is classified as a Cyclization. Most of the rearrangement trajectories started with an OH radical adding at carbons C2 and C4 and are classified as AC2R and AC3R (see Table 2). These sites result in more rearrangement, because the nascent addition products are more highly energized due to chemical activation. Only one trajectory was categorized as AC4R and the mechanism for this trajectory is given in the Supporting Information.

Cyclization mostly produced three-membered rings, but a four-

membered ring was produced by one trajectory. Baldwin[45] concluded that the ring closure forming a four-membered ring is not favorable. As in a previous study,[23] three-membered rings are produced by formation of a bond between the terminal radical center and the inner carbon of the double bond; the energy barrier for this process is only 4.0 kcal/mol (at B3LYP/6-31G(d) level). Four-membered rings are produced by the formation of a bond between the terminal radical center and the outer carbon of the double bond. The barrier to the formation of a four-membered ring is 32 kcal/mol (calculated using B3LYP/6-31G(d)), which is rather high.[23] Therefore formation of three-membered rings is favored.

Table 5 shows that rearrangement and cyclization yields increase at higher energies. This is also reflected in Table 6, which presents reaction cross sections and rate constants for each mechanism and at each energy. From these results, it is clear that radical addition at sites C1 and C4, are dominant.

Table 6. Reaction cross sections and rate constants of non-dissociative trajectories

Product	E = 30kcal/mol		E = 50kcal/mol	
	Cross section[a]	Rate constant[b]	Cross section	Rate constant
AC1	28.5 ± 1.2	12.2 ± 0.5	31.7 ± 1.2	17.6 ± 0.7
AC2	7.3 ± 0.6	3.2 ± 0.3	6.3 ± 0.2	3.5 ± 0.1
AC3	13.0 ± 0.8	5.6 ± 0.3	12.7 ± 0.8	7.0 ± 0.4
AC4	31.6 ± 1.2	13.6 ± 0.5	35.4 ± 1.3	19.6 ± 0.7
AC2R	2.4 ± 0.3	1.0 ± 0.1	3.8 ± 1.0	2.1 ± 0.6
AC3R	1.2 ± 0.2	0.5 ± 0.1	1.6 ± 0.3	0.9 ± 0.2
Cyclization	0.6 ± 0.2	0.2 ± 0.1	1.0 ± 0.2	0.6 ± 0.1

[a]Units of 10^{-17} cm^2; statistical errors are one standard deviation.
[b]Units of 10^{-11} cm^3 $molecule^{-1}$ s^{-1}; statistical errors are one standard deviation.

H-Atom Abstraction and Substitution

Almost all dissociative trajectories proceed by direct H-atom abstraction yielding an H_2O molecule. In this type of reaction, OH radical strikes one of the hydrogens of isoprene and abstracts it to form a water molecule. This type of H atom abstraction reaction accounts for 95.85% of all dissociative trajectories at 30 kcal/mol and 91.84% of those at 50 kcal/mol. Table 7 shows the number and percentage of H atom abstraction trajectories. The reactions are classified as DH1, DH3, or DH5 for initial direct attack on hydrogen atoms at the C1, C3, and C4 sites, respectively.

Inspection of Table 7 shows that the most H atom abstractions are of type DH5, probably because the C-H bonds at that site are weaker due to resonance stabilization of the radical product (Figure 7) and because there are two H-atoms at that site. On a per-H-atom basis, however, reactions of types DH3 and DH5 are the most probable. Table 8 gives cross sections and rate constants for each type of H atom abstraction reaction.

Table 7. The number and percentage of H atom abstraction trajectories of each site among reactive trajectories

Abstraction site	E = 30kcal/mol	E = 50kcal/mol
H1	67 (0.7±0.1) [a]	111 (1.1±0.1)
H3	78 (0.8±0.1)	94 (0.9±0.1)
H4	48 (0.5±0.1)	96 (1.0±0.1)
H5	153 (1.5±0.1)	273 (2.7±0.2)
Total	346 (3.4±0.2)	574 (5.7±0.2)

[a] The percentage is given in parentheses; statistical errors are one standard deviation.

Table 8. Cross sections and rate constants of hydrogen abstraction reactions at each energy value

Product	E = 30kcal/mol		E = 50kcal/mol	
	Cross section[a]	Rate constant[b]	Cross section	Rate constant
DH1 + H_2O	3.4±0.4	1.5±0.2	5.5±0.5	3.0 ±0.3
DH3 + H_2O	3.9±0.4	1.7±0.2	4.7±0.5	2.6±0.3
DH4 + H_2O	2.4±0.3	1.0±0.1	4.8±0.5	2.7±0.3
DH5 + H_2O	7.6±0.6	3.3±0.3	13.5±0.8	7.5±0.5
Total	17.3±0.9	7.5±0.4	28.5±1.2	15.8±0.6

[a]Units are in 10^{-17} cm^2; statistical errors are one standard deviation.
[b]Units are in 10^{-11} cm^3 $molecule^{-1}$ s^{-1}; statistical errors are one standard deviation.

H-atom substitution reactions occur when the OH radical first collides at any site on isoprene and reacts to produce a free hydrogen atom. This is best visualized as a two-step process: addition of the H-atom to a double bond in isoprene, followed by unimolecular dissociation of the chemically activated adduct. This reaction occurred more often at 50 kcal/mol energy. Cross sections are 5.03×10^{-19} cm^2 at 30 kcal/mol energy and 2.32×10^{-16} cm^2 at 50 kcal/mol energy. Thus the rate of substitution reactions is a very strong function of energy, probably due to the high energy requirements of the process.

Other dissociative trajectories can be classified as methyl substitutions, ethene radical eliminations, and other minor channels. These are listed in the Supporting Information. As in the case of H-atom substitution, these reactions are best described as chemical activation processes.

These trajectories were also classified further as "shattering" and "non-shattering". Shattering refers to dissociation that occurs very quickly: within one or two vibrational periods. If the first dissociation occurs within 0.4 ps after collision, the trajectory was classified as a shattering.[48,49] Non-shattering refers to dissociation that occurs after many vibrational periods. In this case, one may assume that substantial intramolecular vibrational energy redistribution (IVR)[46,47] has occurred and statistical rate theory may provide a reasonably accurate estimate of the lifetime of the excited species.

As shown in Table 9, shattering occurred in more than 90% of reactive trajectories. At higher energy (E= 50kcal/mol) the fraction of shattering and non-shattering trajectories increased, but the latter increased more, proportionately. The reason for this difference is difficult to identify, but it may be related to differing fractions of the energy tied up by conservation of angular momentum. In some of the dissociative trajectories, fragmentation occurred after cyclization and rearrangement. All such

trajectories were non-shattering, suggesting that these subsequent rearrangements required more time for IVR and subsequent reaction.

Table 9. The percentage of non-shattering/shattering trajectories among dissociative trajectories [a]

Reaction	E = 30kcal/mol		E = 50kcal/mol	
	Non-shattering	Shattering	Non-shattering	Shattering
Dissociation	3.9±1.0	96.1±1.0	8.1±1.1	91.9±1.1

[a] These are out of 361 (E = 30kcal/mol) and 625 (E = 50kcal/mol) trajectories; statistical errors are one standard deviation.

Thermal Simulations at 300 K

A total of 10938 trajectories were run with sampling from a 300K Boltzmann distribution of relative translational energy. In these trajectories, the reaction probability was very low and all reactive trajectories were OH additions to the carbon-carbon double bonds of isoprene. Table 10 shows the numbers and percentages of trajectories, and the rate constants derived from them. The branching ratios are presented in Table 11, along with results from previous studies.[3,5,13,14,51-59] From the present data, formation of AC1 and AC4 occurred much more often than AC2 and AC3, as was also observed in the simulations at high energies. The total rate constant at 300 K

for AC1-AC4 was found to be 1.29×10^{-10} cm^3 $molecules^{-1}$ s^{-1}, which is consistent with the values ranging from 0.74×10^{-10} to 1.08×10^{-10} cm^3 $molecules^{-1}$ s^{-1} found in the theoretical and experimental studies cited above. This is true despite the fact that the statistical errors are large due to the low probabilities.[50]

Table 10. Free radical addition statistics.

Association site	Number of trajectories	Rate constant (10^{-11} cm^3 $molecules^{-1}$ s^{-1})
AC1	23 (0.21±0.04) [a]	7.2±1.5
AC2	4 (0.04±0.02)	1.3±0.6
AC3	1 (0.01±0.01)	0.3±0.3
AC4	13 (0.12±0.03)	4.3±1.2
Total	41 (0.38±0.06)	12.9±2.0

[a] The percentage is given in parentheses; statistical errors are one standard deviation.

Table 11. Branching ratios among the isoprene-OH radical adducts.

Association site	This work	Previous work[a]	Previous work[b]	Previous work[c]
AC1	0.56	0.67	0.56	0.59
AC2	0.10	0.02	0.02	0.047
AC3	0.02	0.02	0.05	0.047
AC4	0.32	0.29	0.37	0.31

[a] ref. 5.
[b] ref. 11,14.
[c] ref. 11, 60.

4. Summary and Conclusions

Direct dynamics simulations were used to investigate the detailed mechanisms of isoprene + OH. The MSINDO method was used to compute forces and energies on-the-fly and was compared with single point energies of dominant products calculated by the CBS-QB3 and G3B3 methods using UB3LYP/6-311+G(d,p) optimized geometries. In the simulations, all trajectories were classified according to reaction outcomes. Cross sections and rate constants were calculated from the reaction probabilities.

The reactions were first grouped in two types; non-dissociative and dissociative. The most probable reaction type is the addition of OH radical

to the double-bonded carbons of isoprene, resulting in four hydroxyl alkyl radicals (AC1-AC4). Products AC1 and AC4 are energetically more stable than AC2 and AC3 because of allylic stabilization. Rearrangement reactions occurred after OH radical addition at the internal carbon sites (C2 and C3). The major dissociative reaction type is direct hydrogen abstractions to form water and a free radical. Among the abstraction sites, DH3 and DH5 were dominant, due to the weak C–H bonds resulting from resonance stabilization of the product free radicals. At higher energy (50kcal/mol), reactions with more complicated mechanisms occurred, including rearrangements, cyclizations, substitutions, and dissociations.

Trajectories that simulated reaction at 300K resulted in radical addition reactions, exclusively. This result is consistent with previous studies, which have found that this type of reaction is the only one that is important under atmospheric conditions.

References

1. J. Roy, T. D. Sharkey, E. A. Holland, *Trace gas emissions by plants*, Academic Press, San Diego, **1991**.
2. J. H. Seinfeld, S. N. Pandis, *Atmospheric chemistry and physics: from air pollution to climate change*,John Wiley & Sons, New York, **2012**.
3. J. G. Calvert, R. Atkinson, J. Kerr, S. Madronich, G. Moortgat, Wallington, G.Yarwood, *The mechanisms of atmospheric oxidation of the alkenes*,Oxford University Press, New York, **2000**.
4. W. Lei, R. Zhang, W. S. McGivern, A. Derecskei-Kovacs, S. W. North, *J. Phys. Chem. A* **2001**, *105*, 471.
5. E. E. Greenwald, S. W. North, Y. Georgievskii, S. J. Klippenstein, *J. Phys. Chem. A* **2007***, 111*, 5582.
6. M. Keller, M. Lerdau, *Global Biogeochem. Cycles* **1999**, *13*, 19.
7. A. Guenther, C. N. Hewitt, D. Erickson, R. Fall, C. Geron, T. Graedel, P. Harley, L. Klinger, M. Lerdau, W. McKay, *J. Geophys. Res.* **1995**, *100*, 8873.
8. I. Suh, W. Lei, R. Zhang, *J. Phys. Chem. A***2001***, 105*, 6471.
9. L. Whalley, D. Stone, D. Heard, *in Atmospheric and aerosol chemistry*,Springer, **2014**, *339*, p. 55-95 and references there in.
10. M. Karl, H. Dorn, F. Holland, R. Koppmann, D. Poppe, L. Rupp, A. Schaub, A. Wahner, *J. Atmos. Chem.* **2006**, *55*, 167.
11. W. Lei, R. Zhang, W. Sean McGivern, A. Derecskei-Kovacs, S. W. North, *Chem. Phys. Lett.* **2000**, *326*, 109.
12. M. E. Jenkin, S. M. Saunders, M. J. Pilling, *Atmos. Environ.* **1997**, *31*,

81.

13. P. Campuzano -Jost, M. B. William *Geophys. Res. Lett.* **2000**, *27*, 693.
14. J. Fan, R. Zhang, *Environ. Chem.* **2004**, *1*, 140.
15. M. Trainer, E. J. Williams, D. Parrish, M. Buhr, E. Allwine, H. Westberg, F. C. Fehsenfeld, S. C. Liu, *Natur.* **1987***, 329*, 705.
16. W. L. Chameides, R. W. Lindsay, J. Richardson, C. S. Kiang, *Science* **1988***, 241*, 1473.
17. J. Zhao, R. Zhang, E. C. Fortner, S. W. North, *J. Am. Chem. Soc.* **2004***, 126*, 2686.
18. T. L. Nguyen, J. Park, K. Lee, K. Song, J.R. Barker, *J. Phys. Chem. A* **2011***, 115*, 4894.
19. J. H. Park, *Study of the mechanisms and reaction rates for NO_3 +C_2H_4 reactionintheair,*Master's Thesis, Korea National University of Education, **2010**.
20. M. P. Rissanen, A. J. Eskola, T. L. Nguyen, J. R. Barker, J. Liu, J. Liu, E. Halme, R. S. Timonen, *J. Phys. Chem. A* **2014**,*118*, 2176.
21. J. C. Yoon, *A Study on the mechanism of tropospheric reactions of the nitrate radical with propene,* Master's Thesis, Korea National University of Eudcation, **2011**.
22. W. S. McGivern, I. Suh, A. D. Clinkenbeard, R. Zhang, S. W. North, *J. Phys. Chem. A* **2000**, *104*, 6609.
23. J. Park, C. G. Jongsma, R. Zhang, S. W. North, *Phys. Chem. Chem. Phys.* **2003**, *5*, 3638.
24. G. H. Peslherbe, H. Wang, W. L. Hase, *Advances in Chemical Physics:*

Monte Carlo Methods in Chemical Physics **2007**, *105*, 171.

25. W. L. Hase, R. J. Duchovic, X. Hu, A. Komornicki, K. F. Lim, D. Lu, G. H. Peslherbe, K. N. Swamy, S. R. Vande Linde, A. Varandas, H. Wang, R. J. Wolf, VENUS, A General Chemical Dynamics Computer Program, *Quantum Chemistry Program Exchange (QCPE) Bulletin* **1996**, *16*, 671.
26. T. Bredow, K. Jug, *Theoret. Chem. Acc*. **2005**, *113*, 1, and references therein.
27. J. J. P. Stewart, *Stewart Computational Chemistry*, MOPAC2009, Colorado Springs, CO, USA, **2008**.
28. L. Verlet, *Phys. Rev.* **1967**, *159*, 98.
29. M. J. Frisch, G. W. Trucks, H. B. Schlegel, G. E. Scuseria, M. A. Robb, J. R. Cheeseman, G. Scalmani, V. Barone, B. Mennucci, G. A. Petersson, H. Nakatsuji, M. Caricato, X. Li, H. P. Hratchian, A. F. Izmaylov, J. Bloino, G. Zheng, J. L. Sonnenberg, M. Hada, M. Ehara, K.Toyota, R. Fukuda, J. Hasegawa, M. Ishida, T. Nakajima, Y. Honda, O. Kitao, H. Nakai, T. Vreven, J. A. Montgomery Jr., J. E. Peralta, F. Ogliaro, M. Bearpark, J. J. Heyd, E. Brothers, K. N. Kudin, V. N. Staroverov, R. Kobayashi, J. Normand, K. Raghavachari, A. Rendell, J. C. Burant, S. S. Iyengar, J. Tomasi, M. Cossi, N. Rega, J. M. Millam, M. Klene, J. E. Knox, J. B.Cross, V. Bakken, C. Adamo, J. Jaramillo, R. E. Gomperts, O. Stratmann, A. J. Yazyev, R. Austin, C. Cammi, J. W. Pomelli, R. Ochterski, R. L. Martin, K. Morokuma, V. G. Zakrzewski, G. A. Voth, P. Salvador, J. J. Dannenberg, S. Dapprich, A. D. Daniels, O. Farkas, J. B. Foresman, J. V. Ortiz, J. Cioslowski, D. J. Fox, *Gaussian09*, revision D.1, *Gaussian, Inc., Wallingford CT*, **2009**.

30. J. I. Steinfeld, J. S. Francisco, W. L. Hase, *Chemical kinetics and dynamics, second edition*, Prentice-Hall, New Jersey, **1999**.
31. J. Park, C. G. Jongsma, R. Zhang, S. W. North, *J. Phys. Chem. A* **2004**, *108*, 10688.
32. T. Karl, A. Guenther, A. Turnipseed, G. Tyndall, P. Artaxo, S. Martin, *Atmos. Chem. Phys.* **2009**, *9*, 7753.
33. J. A. Montgomery Jr., M. J. Frisch, J. W. Ochterski, G. A. Petersson, *J. Chem. Phys.* **1999**, *110*, 2822.
34. A.G. Baboul, L.A. Curtiss, P.C. Redfern, K. Raghavachari. *J. Chem. Phys.* **1999**, *110*, 7650.
35. K. Park, K. Song, W. L. Hase, *Int. J. Mass Spectrom.* **2007**, *265*, 326.
36. P. S. Stevens, E. Seymour, Z. Li, *J. Phys. Chem. A* **2000**, *104*, 5989.
37. L. Sun, K. Park, K.Song, D. W. Setser, W. L. Hase, *J. Chem. Phys.* **2006**, 124, 064313.
38. W. L. Hase, K. Song, M. S. Gordon, *Computing in Science & Engineering* **2003**, *5*, 36.
39. G. Park, *Direct dynamics studies of chemical reactions,* Master's Thesis, Korea National University of Eudcation, **2007**.
40. L. Sun, K. Song, W. L. Hase, *Science* **2002**, *296*, 875.
41. M. Franc4isco-Márquez, J. R. Alvarez-Idaboy, A. Galano, A. Vivier-Bunge, *Phys. Chem. Chem. Phys*. **2003**, *5*, 1392.
42. E. E. Greenwald, B. Ghosh, K. C. Anderson, K. S. Dooley, P. Zou, T. Selby, D. L. Osborn, G. Meloni, C. A. Taatjes, F. Goulay, *J. Phys. Chem. A* **2009**, *114*, 904.
43. J. Park, *Experimental and theoretical studies of isoprene oxidation*

initiated by hydroxyl radical, Doctor's thesis, Texas A&M University, **2004**.

44. M. Karl, T. Brauers, H. Dorn, F. Holland, M. Komenda, D. Poppe, F. Rohrer, L. Rupp, A. Schaub, A. Wahner, *Geophys. Res. Lett.* **2004***, 31, 5*.
45. J. E. Baldwin, *J. Chem. Soc. Chem. Comm.* **1976**, 734.
46. A. L. Kaledin, W. H. Miller, *J. Chem. Phys.* **2003***, 118*, 7174.
47. A. L. Kaledin, W. H. Miller, *J. Chem. Phys.* **2003***, 119*, 3078.
48. S. Lee, *Effect of termini substitution in the CID of protonated penta- and octaglycine,*Master's Thesis, Korea National University of Education, **2013**.
49. T. Baer, W. L. Hase, *Unimolecular reaction dynamics,* Oxford Univ. Press, New York, **1996**.
50. H. A. Laitinen, W. E. Harris, *Chemical Analysis (2nd ed.)*, McGraw-Hill, New York, **1975***,* 569.
51. S. Sander, R. Friedl, J. Barker, D. Golden, M. Kurylo, G. Moortgat, P. Wine, J. Abbatt, J. Burkholder, C. Kolb, R. Huie, V. Orkin, *Chemical kinetics and photochemical data for use in atmospheric studies, NASA, Supplement to evaluation 17*, JPL, Pasadena, CA, **2011***, 10-6*.
52. D. B. Atkinson, M. A. Smith, *J. Phys. Chem.* **1994***, 98*, 5797.
53. R. Atkinson, *Chem. Rev.* **1986**, *86*, 69.
54. R. Atkinson, S. M. Aschmann, A. M. Winer, J. N. Pitts, *Int. J. Chem. Kinet.* **1982**, *14*, 507.
55. R. Atkinson, S. M. Aschmann, *Int. J. Chem. Kinet.* **1984**, *16*, 1175.
56. T. E. Kleindienst, G. W. Harris, J. N. Pitts, *Environ. Sci. Technol.* **1982**,

16, 844.

57. S. McKeen, G. Mount, F. Eisele, E. Williams, J. Harder, P. Goldan, W. Kuster, S. Liu, K. Baumann, D. Tanner, *J. Geophys. Res*. **1997**, *102*, 6467.
58. E. C. Tuazon, R. Atkinson, *Int. J. Chem. Kinet.* **1990**, *22*, 1221.
59. R. A. Cox, R. G. Derwent, M. R. Williams, *Environ. Sci. Technol.* **1980**, *14*, 57.
60. M. E. Jenkin, G. D. Hayman, *J. Chem. Soc. Faraday Trans*. **1995**, *91*, 1911.

ABSTRACT

The products and mechanisms active in the reaction isoprene + OH reaction were investigated using the direct dynamics method. High energies were used in order to identify every possible reaction channel. The trajectories were classified as dissociative and non-dissociative, depending on whether fragmentation occurred during the 4 ps time window of the simulations. The non-dissociative trajectories were further classified as radical additions, rearrangements, and cyclizations. The most dominant category was the addition of OH to the carbons of isoprene to form adducts. Some adducts react further by isomerization and cyclization. The dissociative trajectories were classified as hydrogen abstractions, substitutions, and eliminations. Among these, the dominant category was direct hydrogen abstraction to produce H_2O and a free radical. At higher energies, more reaction was observed. In simulations at 300K, the only reaction category observed was OH addition to the double bonds in isoprene to form adducts.